Acta Crystallographica Section F
Structural Biology and Crystallization Communications
ISSN 1744-3091

Crystallization and preliminary X-ray diffraction analysis of the wild-type haloalkane dehalogenase DhaA and its variant DhaA13 complexed with different ligands

Alena Stsiapanava,[a] Radka Chaloupkova,[b] Andrea Fortova,[b] Jiri Brynda,[c] Manfred S. Weiss,[d] Jiri Damborsky[b] and Ivana Kuta Smatanova[a,e]*

[a]Institute of Physical Biology, University of South Bohemia Ceske Budejovice, Zamek 136, CZ-373 33 Nove Hrady, Czech Republic, [b]Loschmidt Laboratories, Department of Experimental Biology and Research Centre for Toxic Compounds in the Environment, Faculty of Science, Masaryk University, Kamenice 5/A4, CZ-62 500 Brno, Czech Republic, [c]Institute of Molecular Genetics, Academy of Science of the Czech Republic, Flemingovo nam. 2, CZ-166 37 Prague 6, Czech Republic, [d]Macromolecular Crystallography (BESSY-MX), Helmholtz-Zentrum Berlin, Albert-Einstein-Strasse 15, D-12489 Berlin, Germany, and [e]Institute of Systems Biology and Ecology, v.v.i., Academy of Science of the Czech Republic, Zamek 136, CZ-373 33 Nove Hrady, Czech Republic

Correspondence e-mail: ivanaks@seznam.cz

Received 22 October 2010
Accepted 7 December 2010

Haloalkane dehalogenases make up an important class of hydrolytic enzymes which catalyse the cleavage of carbon–halogen bonds in halogenated aliphatic compounds. There is growing interest in these enzymes owing to their potential use in environmental and industrial applications. The haloalkane dehalogenase DhaA from *Rhodococcus rhodochrous* NCIMB 13064 can slowly detoxify the industrial pollutant 1,2,3-trichloropropane (TCP). Structural analysis of this enzyme complexed with target ligands was conducted in order to obtain detailed information about the structural limitations of its catalytic properties. In this study, the crystallization and preliminary X-ray analysis of complexes of wild-type DhaA with 2-propanol and with TCP and of complexes of the catalytically inactive variant DhaA13 with the dye coumarin and with TCP are described. The crystals of wild-type DhaA were plate-shaped and belonged to the triclinic space group $P1$, while the variant DhaA13 can form prism-shaped crystals belonging to the orthorhombic space group $P2_12_12_1$ as well as plate-shaped crystals belonging to the triclinic space group $P1$. Diffraction data for crystals of wild-type DhaA grown from crystallization solutions with different concentrations of 2-propanol were collected to 1.70 and 1.26 Å resolution, respectively. A prism-shaped crystal of DhaA13 complexed with TCP and a plate-shaped crystal of the same variant complexed with the dye coumarin diffracted X-rays to 1.60 and 1.33 Å resolution, respectively. A crystal of wild-type DhaA and a plate-shaped crystal of DhaA13, both complexed with TCP, diffracted to atomic resolutions of 1.04 and 0.97 Å, respectively.

1. Introduction

Haloalkane dehalogenases (EC 3.8.1.5) belong to the α/β-hydrolase superfamily of enzymes (Ollis *et al.*, 1992; Nardini & Dijsktra, 1999) and catalyze the hydrolytic conversion of a broad spectrum of halogenated aliphatic hydrocarbons. The dehalogenation reaction that is catalyzed by these enzymes proceeds *via* covalent alkyl-enzyme intermediates in two consecutive chemical steps: (i) the formation of the intermediate by bimolecular nucleophilic substitution and (ii) the hydrolysis of the intermediate by nucleophilic addition (Janssen, 2004). The three products of the reaction are an alcohol, a halide ion and a proton. Haloalkane dehalogenases (HLDs) catalyze reactions of great environmental and biotechnological significance and find application in the bioremediation of various pollutants (Stucki & Thuer, 1995), the decontamination of warfare agents (Prokop *et al.*, 2005, 2006), the biosensing of toxic compounds (Campbell *et al.*, 2006; Bidmanova *et al.*, 2010) and the biosynthesis of optically pure compounds (Prokop *et al.*, 2004, 2010; Janssen, 2007).

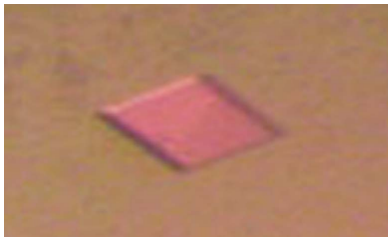

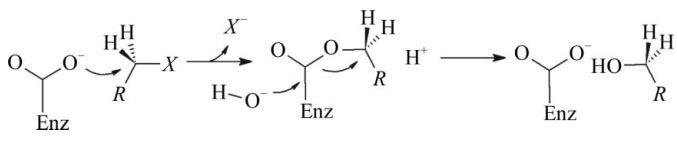

Figure 1
Reaction mechanism of the haloalkane dehalogenases. Enz, enzyme.

The catalytic residues of DhaA comprise a catalytic pentad: a nucleophile, a base, a catalytic acid and a pair of halide-stabilizing residues: Asp–His–Glu + Asn–Trp. Catalysis proceeds *via* the nucleophilic attack of the carboxylate O atom of an aspartate group on the C atom of the substrate, yielding the displacement of the halogen atom as a halide, and the formation of a covalent alkyl-enzyme intermediate (Fig. 1). The alkyl-enzyme intermediate is subsequently hydrolyzed by a water molecule that is activated by a histidine. A catalytic acid stabilizes the charge developed on the imidazole ring of the His during the hydrolytic reaction. Since the formation of enzyme–substrate complexes inside a crystal is often difficult, the variant DhaA13, in which the catalytic histidine was replaced by a phenylalanine, was constructed so that the catalytic cycle would be terminated after the first reaction step at the stage of the alkyl-enzyme intermediate.

In this work, we report the crystallization and initial X-ray diffraction characterization of wild-type DhaA and its variant DhaA13 in complex with the environmental pollutant trichloropropane (TCP). Furthermore, we describe the crystallization of DhaA13 in complex with the fluorescent dye coumarin. The complex with coumarin, in which the dye is specifically located in the tunnel mouth of the DhaA13 enzyme, was used in time-resolved fluorescence spectroscopy to monitor the hydration, accessibility and mobility of the dye and its microenvironment in the protein (Jesenska *et al.*, 2009). Finally, we studied the complex of wild-type DhaA with 2-propanol. As the technological utility of enzymes can be improved greatly by using them in organic co-solvents, rather than in their natural aqueous reaction media (Klibanov, 2001; Carrea & Riva, 2000), a systematic study of the effects of various organic co-solvents on the structure and activity of three different HLDs was initiated (Stepankova *et al.*, unpublished work). Here, we describe the complexes of wild-type DhaA with two different concentrations of 2-propanol to investigate the ability of the solvent to access the enzyme active site and its effect on the enzyme structure.

2. Materials and methods

2.1. Site-directed mutagenesis, protein expression and purification

Wild-type DhaA was expressed in *Escherichia coli* BL21 cells and was purified using immobilized metal-affinity chromatography as described previously (Pavlova *et al.*, 2009). The recombinant gene carrying the single point mutation H272F was obtained using the QuikChange Site-Directed Mutagenesis Kit (Strategene, La Jolla, USA) according to the manufacturer's instructions. The resulting DhaA13 protein variant was also overexpressed in *E. coli* BL21 cells and purified using the same protocol as for the wild type (Jesenska *et al.*, 2009). The active fractions of both proteins were pooled and dialyzed overnight against 50 m*M* Tris–HCl buffer pH 7.5. Protein concentrations were determined by the method of Bradford (1976). The purity and size of both enzymes were verified by SDS–PAGE.

2.2. Crystallization

All crystallization experiments were performed at 277 K in Emerald BioStructures CombiClover Crystallization Plates (Emerald BioSystems, Bainbridge Island, USA) using the sitting-drop vapour-diffusion method (Ducruix & Giegé, 1999).

Wild-type DhaA protein was crystallized at a concentration of 10 mg ml^{-1} in 50 m*M* Tris–HCl buffer pH 7.5. Colourless crystals with dimensions of 0.17 × 0.05 × 0.03 mm (Fig. 2*a*) were obtained within 5 d in drops consisting of protein solution plus precipitant solution composed of 25%(*w*/*v*) PEG 4000, 6%(*v*/*v*) 2-propanol and 100 m*M* sodium acetate salt. A second form of wild-type DhaA crystals with similar dimensions of 0.19 × 0.03 × 0.03 mm (Fig. 2*b*) grew within 5 d from crystallization solution consisting of 24%(*w*/*v*) PEG 4000, 11%(*v*/*v*) 2-propanol and 100 m*M* sodium acetate salt. Plate-shaped crystals of wild-type DhaA appeared in 2 d and grew in 7 d to maximum dimensions of 0.23 × 0.1 × 0.02 mm (Fig. 2*c*) from a solution consisting of 39%(*w*/*v*) PEG 4000, 6%(*v*/*v*) TCP and

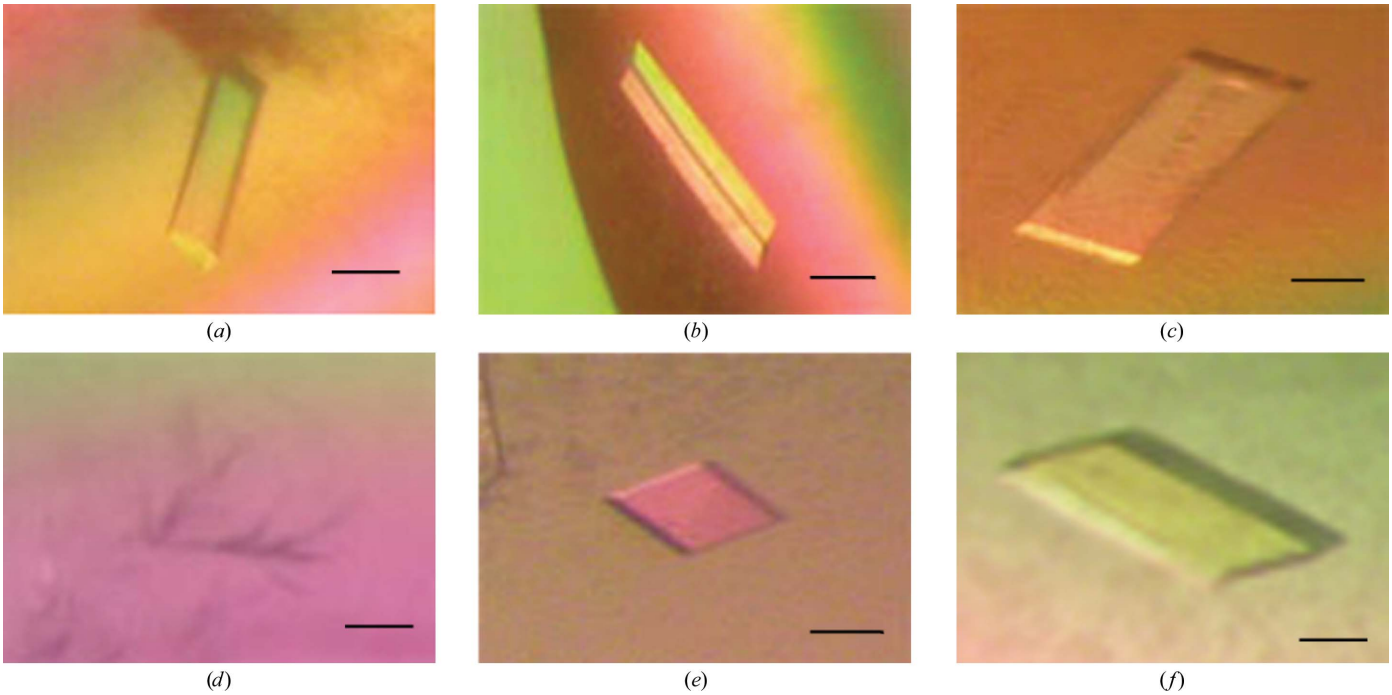

Figure 2
Crystals of wild-type DhaA isolated from *R. rhodochrous* NCIMB 13064 (*a*) grown from solution containing 6%(*v*/*v*) 2-propanol, (*b*) grown from solution containing 11%(*v*/*v*) 2-propanol and (*c*) grown from solution containing 6%(*v*/*v*) TCP. (*d*) Microcrystals, (*e*) plate-shaped crystals grown using the microseeding method and (*f*) prism-shaped crystals of the variant DhaA13. The scale bar represents 70 µm.

Table 1
Data-collection statistics for wild-type DhaA crystals.

Values in parentheses are for the highest resolution shell.

Ligand	2-Propanol†	2-Propanol‡	TCP
Radiation source	Bruker FR591	X12, DESY	14.1, BESSY
Detector	MAR345	225 mm MAR Mosaic CCD	225 mm MAR Mosaic CCD
Wavelength (Å)	1.542	1.033	0.918
No. of images		130§/400¶	380§/380¶/380††
Rotation range per image (°)		1.5§/0.5¶	0.5§/0.5¶/0.5††
Resolution range (Å)	22.94–1.75 (1.84–1.75)	50.0–1.26 (1.31–1.26)	30.0–1.04 (1.14–1.04)
Space group	*P*1	*P*1	*P*1
Unit-cell parameters (Å, °)	a = 42.71, b = 44.51, c = 46.40, α = 115.40, β = 98.10, γ = 109.4	a = 42.65, b = 44.48, c = 46.33, α = 115.39, β = 98.05, γ = 109.4	a = 42.56, b = 44.37, c = 46.30, α = 115.151, β = 97.59, γ = 109.80
Measured reflections	58098	166175	662439
Unique reflections	25072	69951	125718
Multiplicity	2.3	2.4	5.3
Completeness (%)	90.5 (87.4)	94.3 (90.2)	95.6 (89.8)
$R_{\rm merge}$‡‡ (%)	5.0 (30.9)	3.7 (11.3)	8.0 (35.8)
$R_{\rm meas}/R_{\rm r.i.m.}$§§ (%)	6.0 (31.9)	4.5 (15.3)	7.2 (54.8)
$\langle I/\sigma(I)\rangle$	15.0 (3.9)	29.9 (6.8)	17.53 (4.9)

† The concentration of 2-propanol in the crystallization solution was 6%(*v*/*v*). ‡ The concentration of 2-propanol in the crystallization solution was 11%(*v*/*v*). § Low-resolution pass. ¶ High-resolution pass. †† Third pass (change in κ). ‡‡ $R_{\rm merge} = \sum_{hkl}\sum_i |I_i(hkl) - \langle I(hkl)\rangle|/\sum_{hkl}\sum_i I_i(hkl)$, where $I_i(hkl)$ is the intensity of the ith measurement of reflection hkl and $\langle I(hkl)\rangle$ is the average intensity of this reflection. §§ $R_{\rm meas}/R_{\rm r.i.m.} = \sum_{hkl}[N/(N-1)]^{1/2}\sum_i |I_i(hkl) - \langle I(hkl)\rangle|/\sum_{hkl}\sum_i I_i(hkl)$, where N is the redundancy of the observed reflection.

100 m*M* sodium acetate salt. In all three cases, 1 µl protein solution was mixed with an equal volume of crystallization solution and the drops were equilibrated over 700 µl reservoir solution.

Microcrystals of DhaA13 (Fig. 2*d*) were obtained in 2 d by mixing 1 µl protein solution at a concentration of 10 mg ml^{-1} in 50 m*M* Tris–HCl buffer pH 7.5 with 1 µl precipitant solution consisting of 100 m*M* sodium cacodylate pH 6.4, 29%(*w*/*v*) PEG 8000 and 200 m*M* sodium acetate. The microcrystals were optimized by microseeding (Bergfors, 2003).

Small protein crystals from several drops were transferred into 20 µl of a stabilizing solution consisting of 75 m*M* sodium cacodylate pH 6.4, 22%(*w*/*v*) PEG 8000 and 150 m*M* sodium acetate and were stored at 277 K. Before setting up crystallization trials, the stabilizing solution containing crushed protein microcrystals was diluted tenfold. 0.3 µl of the prepared seed solution was added to a drop that had been equilibrated for 1 d consisting of 2 µl protein solution at a concentration of 5 mg ml^{-1} in 50 m*M* Tris–HCl buffer pH 7.5 and 2 µl crystallization solution consisting of 100 m*M* sodium cacodylate pH 6.4, 29%(*w*/*v*) PEG 8000 and 200 m*M* sodium acetate. All drops were equilibrated against 600 µl reservoir solution. After several cycles of microseeding, plate-shaped crystals with dimensions of about of 0.12 × 0.1 × 0.02 mm (Fig. 2*e*) were obtained.

The same crystallization conditions that produced microcrystals of DhaA13 yielded crystals of another shape. Three months after the experiment had been set up, prism-shaped crystals of DhaA13 with dimensions of 0.24 × 0.12 × 0.07 mm (Fig. 2*f*) were observed in the drops.

2.3. Diffraction data collection and processing

The data-collection and processing statistics for wild-type DhaA and DhaA13 in complex with ligands are summarized in Tables 1 and 2, respectively.

2.3.1. Wild-type DhaA with 6%(*v*/*v*) 2-propanol. Diffraction data for wild-type DhaA crystals grown from solution containing 6%(*v*/*v*) 2-propanol were collected on the home diffractometer equipped with a MAR345 image-plate system using a Nonius FR591 rotating-anode generator (Bruker AXS) at the Institute of Molecular Genetics AS CR in Prague (Czech Republic). To ensure complete data, two crystals were flash-cooled to 120 K in a nitrogen stream without additional cryoprotection and were measured in different orientations. The data were scaled and merged together. These crystals diffracted to a resolution of 1.75 Å.

2.3.2. Wild-type DhaA with 11%(*v*/*v*) 2-propanol. Diffraction data from a crystal of wild-type DhaA grown from solution containing 11%(*v*/*v*) 2-propanol were collected on EMBL Hamburg beamline X12 (DESY, Hamburg, Germany) using a MAR CCD 225 mm detector. The crystal was mounted in a nylon loop (Teng, 1990) and flash-cooled in a nitrogen stream at 100 K without additional cryoprotection. Low-resolution and high-resolution passes were collected at crystal-to-detector distances of 300 and 100 mm, respectively. The crystal diffracted to a maximum resolution of 1.26 Å. The data were processed using the *HKL*-2000 program package (Otwinowski & Minor, 1997). The redundancy-independent merging *R* factor ($R_{\rm meas}$ or $R_{\rm r.i.m.}$; Diederichs & Karplus, 1997; Weiss, 2001) was calculated with the *RMERGE* program (Weiss, 2001).

2.3.3. Wild-type DhaA in complex with TCP. A crystal of wild-type DhaA complexed with TCP was soaked for 10 s in a solution consisting of 10%(*v*/*v*) PEG 400 in reservoir solution and was subsequently flash-cooled to 100 K in a nitrogen stream. The crystal diffracted to 1.04 Å resolution and data were collected in three passes on BESSY II beamline 14.1 in Berlin, Germany. Low-resolution and high-resolution passes were recorded at distances of 96.5 and 92 mm, respectively. A third pass was collected after reorienting the crystal by about 30° using the available kappa goniometry, with a crystal-to-detector distance of 92 mm. Images were indexed, integrated and scaled using the *XDS* program package (Kabsch, 1993, 2010*a*,*b*).

2.3.4. DhaA13 variant in complex with TCP (crystal soaked for 3 h). Soaking experiments of DhaA13 crystals with TCP were performed at room temperature. 50 µl TCP was added to the reservoir solution and after 3 h of soaking a crystal without additional cryoprotection was used for diffraction experiments on beamline X12 of the DESY synchrotron (Hamburg, Germany). This crystal diffracted to a maximal resolution of 1.60 Å. The diffraction data set was indexed and integrated with *XDS* and was scaled using *SCALA* from the *CCP*4 program suite (Collaborative Computational Project, Number 4, 1994).

2.3.5. DhaA13 variant in complex with TCP (crystal soaked for 40 h). A crystal of DhaA13 was soaked with TCP at 277 K for 40 h; 50 µl TCP was added to the reservoir solution. This crystal was

Table 2
Data-collection statistics for the DhaA13 crystals.

Values in parentheses are for the highest resolution shell.

Ligand	TCP†	TCP‡	Coumarin dye
Radiation source	X12, DESY	14.1, BESSY	X12, DESY
Detector	225 mm MAR Mosaic CCD	225 mm MAR Mosaic CCD	225 mm MAR Mosaic CCD
Wavelength (Å)	1.033	0.827	1.033
Resolution range (Å)	46.6–1.60 (1.69–1.60)	10.0–0.97 (0.98–0.97)	50.00–1.33 (1.38–1.33)
No. of images	400	180§/180¶/180††	400
Rotation range per image (°)	0.5	1§/1¶/1††	0.5
Space group	$P2_12_12_1$	$P1$	$P1$
Unit-cell parameters (Å, °)	$a = 42.68$, $b = 75.89$, $c = 93.17$, $\alpha = \beta = \gamma = 90$	$a = 42.72$, $b = 44.48$, $c = 46.55$, $\alpha = 115.3$, $\beta = 98.74$, $\gamma = 109.16$	$a = 42.64$, $b = 44.41$, $c = 46.32$, $\alpha = 115.33$, $\beta = 98.56$, $\gamma = 109.36$
Measured reflections	323981	575134	124812
Unique reflections	40857	159375	58738
Multiplicity	7.9	3.6	2.1
Completeness (%)	99.9 (99.6)	97.6 (93.7)	93.8 (81.1)
$R_{\rm merge}$‡‡ (%)	10.3 (63.1)	10.5 (83.4)	3.3 (11.4)
$R_{\rm meas}/R_{\rm r.i.m.}$§§ (%)	11.0 (67.6)	6.7 (67.4)	4.4 (15.6)
$\langle I/\sigma(I)\rangle$	13.6 (3.2)	14.74 (2.2)	27.9 (5.3)

† Soaked for 3 h. ‡ Soaked for 40 h. § Low-resolution pass. ¶ High-resolution pass. †† Third pass (change in κ). ‡‡ $R_{\rm merge} = \sum_{hkl}\sum_i |I_i(hkl) - \langle I(hkl)\rangle|/\sum_{hkl}\sum_i I_i(hkl)$, where $I_i(hkl)$ is the intensity of the ith measurement of reflection hkl and $\langle I(hkl)\rangle$ is the average intensity of this reflection. §§ $R_{\rm meas}/R_{\rm r.i.m.} = \sum_{hkl}[N/(N-1)]^{1/2}\sum_i |I_i(hkl) - \langle I(hkl)\rangle|/\sum_{hkl}\sum_i I_i(hkl)$, where N is the redundancy of the observed reflection.

mounted in a nylon loop and flash-cooled to 100 K in a nitrogen stream without additional cryoprotection. Diffraction data were collected to 0.97 Å from the soaked DhaA13 crystal in three passes on beamline 14.1 at the BESSY II synchrotron in Berlin: low-resolution and high-resolution passes with the MAR CCD detector set to 180 and 93 mm, respectively, and a third pass in which the κ angle was changed to 114° with a crystal-to-detector distance of 93 mm. The data sets for DhaA13 in complex with TCP were indexed, integrated and scaled using the *XDS* program package.

2.3.6. DhaA13 variant in complex with coumarin dye. To obtain the complex of DhaA13 with coumarin dye, 0.5 µl 10 m*M* HaloTag Coumarin Ligand (Promega Corporation, Madison, USA) was added to drops containing crystals for 10 min. Most of the crystals cracked during the soaking test. A diffraction data set from an intact crystal was collected to a resolution of 1.33 Å on beamline X12, DESY, Hamburg. The data were processed with *HKL*-2000 and $R_{\rm meas}/R_{\rm r.i.m.}$ was obtained using the program *RMERGE*.

Single crystals of wild-type DhaA obtained from solutions containing 11%(*v*/*v*) 2-propanol and 6%(*v*/*v*) TCP were used for synchrotron diffraction measurements and diffracted to resolutions of 1.26 and 1.04 Å, respectively. The diffraction patterns indicated that the two crystals both belonged to the triclinic space group *P*1. For completeness, the triclinic crystal of DhaA in complex with TCP was reoriented during data collection by changing the κ angle of the goniostat (Dauter, 1999). Assuming the presence of one molecule in the asymmetric unit yields Matthews coefficients ($V_{\rm M}$) of 2.00 and 1.99 Å^3 Da^{-1} with 38.5 and 38.3% solvent content for the crystals of wild-type DhaA grown from crystallization solutions containing 11%(*v*/*v*) 2-propanol and 6%(*v*/*v*) TCP, respectively.

All data-collection and processing statistics are given in Table 1. Based on commonly accepted quality indicators such as $R_{\rm merge}$, $R_{\rm meas}/R_{\rm r.i.m.}$ and $\langle I/\sigma(I)\rangle$, the data sets show above-average quality. Despite the low-symmetry space group *P*1, the high-resolution shells of the data sets show completeness close to or above 90%.

3. Results and discussion

3.1. Crystallization and characterization of wild-type DhaA

The crystallization conditions that were successfully used for the previously studied mutants DhaA14 and DhaA15 (Stsiapanava *et al.*, 2008) were applied to wild-type DhaA. Variation of the 2-propanol content in the crystallization mixture resulted in crystals of wild-type DhaA from solutions containing 6%(*v*/*v*) and 11%(*v*/*v*) 2-propanol. Increasing the PEG concentration in the crystallization mixture and replacing 2-propanol by TCP, which is a known substrate of this enzyme, resulted in the growth of wild-type DhaA plate-shaped crystals which differed in morphology from the crystals grown from solutions containing 2-propanol.

Crystals of wild-type DhaA grown from the solution containing 6%(*v*/*v*) 2-propanol were used for data collection at a home source and a complete data set was collected to 1.75 Å resolution. The crystals belonged to the triclinic space group *P*1. Based on the molecular weight of the protein (34 kDa, including the six amino acids of the histidine tag) and the volume of the asymmetric unit, the Matthews coefficient ($V_{\rm M}$; Matthews, 1968) is 2.17 Å^3 Da^{-1} and the solvent content is 43.5%, assuming the presence of one molecule in the asymmetric unit.

3.2. Crystallization and characterization of the DhaA13 variant

Initial crystallization conditions for DhaA13 were screened using Crystal Screen (Hampton Research, Aliso Viejo, USA), PEG-based conditions from the JBScreen Classic Ampoules Mixed kit (Jena Bioscience GmbH, Jena, Germany) and Clear Strategy Screen 1 (Molecular Dimensions Ltd, Suffolk, England). Crystallization of the mutant protein was observed in condition No. 28 of Crystal Screen [100 m*M* sodium cacodylate pH 6.5, 30%(*w*/*v*) PEG 8000 and 200 m*M* sodium acetate]. Optimization of this condition yielded an optimized precipitant solution consisting of 100 m*M* sodium cacodylate pH 6.4, 29%(*w*/*v*) PEG 8000 and 200 m*M* sodium acetate. Microcrystals and crystals of DhaA13 appeared in different drops with the same composition within 2 d and three months, respectively. A stabilizing solution consisting of the components of the reservoir solution at an approximately 75% concentration [75 m*M* sodium cacodylate pH 6.4, 22%(*w*/*v*) PEG 8000 and 150 m*M* sodium acetate] was used to slightly melt the surface of the seeds and resulted in successful microseeding experiments.

A prism-shaped crystal of DhaA13 soaked with TCP for 3 h diffracted X-rays to a resolution of 1.60 Å. The crystal belonged to the orthorhombic space group $P2_12_12_1$. The Matthews coefficient

(V_M) of 2.21 Å^3 Da^{-1} and the solvent content of 44.5% are consistent with the presence of one molecule in the asymmetric unit.

A plate-shaped crystal of DhaA13 was soaked with TCP for 40 h and diffracted to 0.97 Å resolution. Another DhaA13 crystal of the same shape was soaked with coumarin dye for 10 min and data were collected to a resolution of 1.33 Å. Data sets were processed in the triclinic space group *P*1, with one molecule in the asymmetric unit in both cases. The calculated value of the Matthews coefficient (V_M) for DhaA13 in complex with TCP is 2.08 Å^3 Da^{-1} and the solvent content is 41.0%. The Matthews coefficient (V_M) for DhaA13 in complex with coumarin dye was calculated as 2.06 Å^3 Da^{-1}, which corresponds to a solvent content of 40.4%.

The data-collection and processing statistics for the DhaA13 crystals are listed in Table 2. Similarly to the case of the wild-type DhaA protein crystals, the orthorhombic and triclinic crystals of DhaA13 demonstrated high completeness and good characteristics for the *R* factors and $\langle I/\sigma(I)\rangle$. The high *R* factors of triclinic DhaA13 in complex with TCP in the outer resolution shells are a consequence of both counting statistics and slowly accumulating radiation damage (Diederichs, 2006). Nevertheless, it was essential to include the complete third pass in the final data set in order to ensure high completeness.

3.3. Preliminary determination of protein structures

The structures of wild-type DhaA and variant DhaA13 were solved by molecular replacement with the program *MOLREP* (Vagin & Teplyakov, 2010) using the coordinates of *R. rhodochrous* haloalkane dehalogenase (PDB code 3fbw; Stsiapanava *et al.*, 2010) as a search model. Structure refinement of the presented proteins and their complexes are currently in progress.

The authors would like express their thanks to the technician Monika Strakova (Loschmidt Laboratories, Masaryk University, Brno) for purification of the proteins and to Paul Tucker (EMBL Outstation, Hamburg), Uwe Mueller and Jörg Schulze (BESSY, Berlin) for their help during data collection. We thank the EMBL for access to the X12 beamline at the DORIS storage ring of DESY in Hamburg. We would like to acknowledge support through the EC under the ELISA grant (agreement No. 226716) for access to BESSY II. This work is supported by the Ministry of Education of the Czech Republic (LC06010, MSM6007665808, MSM0021622412, MSM0021622413, CZ.1.05/2.1.00/01.0001), the Academy of Sciences of the Czech Republic (AV0Z60870520, IAA401630901) and the Czech Science Foundation (310/09/1407).

References

Bergfors, T. M. (2003). *J. Struct. Biol.* **142**, 66–76.
Bidmanova, S., Chaloupkova, R., Damborsky, J. & Prokop, Z. (2010). *Anal. Bioanal. Chem.* **398**, 1891–1898.
Bradford, M. M. (1976). *Anal. Biochem.* **72**, 248–254.
Campbell, D. W., Muller, C. & Reardon, K. F. (2006). *Biotechnol. Lett.* **28**, 883–887.
Carrea, G. & Riva, S. (2000). *Angew. Chem. Int. Ed.* **39**, 2226–2254.
Collaborative Computational Project, Number 4 (1994). *Acta Cryst.* D**50**, 760–763.
Dauter, Z. (1999). *Acta Cryst.* D**55**, 1703–1717.
Diederichs, K. (2006). *Acta Cryst.* D**62**, 96–101.
Diederichs, K. & Karplus, P. A. (1997). *Nature Struct. Biol.* **4**, 269–275.
Ducruix, A. & Giegé, R. (1999). *Crystallization of Nucleic Acids and Proteins: A Practical Approach*, 2nd ed. Oxford University Press.
Janssen, D. B. (2004). *Curr. Opin. Chem. Biol.* **8**, 150–159.
Janssen, D. B. (2007). *Adv. Appl. Microbiol.* **61**, 233–252.
Jesenska, A., Sykora, J., Olzynska, A., Brezovsky, J., Zdrahal, Z., Damborsky, J. & Hof, M. (2009). *J. Am. Chem. Soc.* **131**, 494–501.
Kabsch, W. (1993). *J. Appl. Cryst.* **26**, 795–800.
Kabsch, W. (2010*a*). *Acta Cryst.* D**66**, 125–132.
Kabsch, W. (2010b). *Acta Cryst.* D**66**, 133–144.
Klibanov, A. M. (2001). *Nature (London)*, **409**, 241–246.
Matthews, B. W. (1968). *J. Mol. Biol.* **33**, 491–497.
Nardini, M. & Dijsktra, B. W. (1999). *Curr. Opin. Struct. Biol.* **9**, 732–737.
Ollis, D. L., Cheah, E., Cygler, M., Dijkstra, B., Frolow, F., Franken, S. M., Harel, M., Remington, S. J., Silman, I., Schrag, J., Sussman, J. L., Verschueren, K. H. G. & Goldman, A. (1992). *Protein Eng.* **5**, 197–211.
Otwinowski, Z. & Minor, W. (1997). *Methods Enzymol.* **276**, 307–326.
Pavlova, M., Klvana, M., Prokop, Z., Chaloupkova, R., Banas, P., Otyepka, M., Wade, R. C., Tsuda, M., Nagata, Y. & Damborsky, J. (2009). *Nature Chem. Biol.* **5**, 727–733.
Prokop, Z., Damborsky, J., Nagata, Y. & Janssen, D. B. (2004). Patent WO 2006/079295 A2.
Prokop, Z., Damborsky, J., Oplustil, F., Jesenska, A. & Nagata, Y. (2005). Patent WO 2006/128390 A1.
Prokop, Z., Oplustil, F., DeFrank, J. & Damborsky, J. (2006). *Biotechnol. J.* **1**, 1370–1380.
Prokop, Z., Sato, Y., Brezovsky, J., Mozga, T., Chaloupkova, R., Koudelakova, T., Jerabek, P., Stepankova, V., Natsume, R., Leeuwen, J. G. E., Janssen, D. B., Florian, J., Nagata, Y., Senda, T. & Damborsky, J. (2010). *Angew. Chem. Int. Ed.* **49**, 6111–6115.
Stsiapanava, A., Dohnalek, J., Gavira, J. A., Kuty, M., Koudelakova, T., Damborsky, J. & Kuta Smatanova, I. (2010). *Acta Cryst.* D**66**, 962–969.
Stsiapanava, A., Koudelakova, T., Lapkouski, M., Pavlova, M., Damborsky, J. & Kuta Smatanova, I. (2008). *Acta Cryst.* F**64**, 137–140.
Stucki, G. & Thuer, M. (1995). *Environ. Sci. Technol.* **29**, 2339–2345.
Teng, T.-Y. (1990). *J. Appl. Cryst.* **23**, 387–391.
Vagin, A. & Teplyakov, A. (2010). *Acta Cryst.* D**66**, 22–25.
Weiss, M. S. (2001). *J. Appl. Cryst.* **34**, 130–135.